Article:
Booth, M, Peel, R, Partanen, R et al. (4 more authors) (2013) Amphipol-encapsulated CuInS/ZnS quantum dots with excellent colloidal stability. RSC Advances, 3 (43). 20559 - 20566. ISSN 2046-2069

https://doi.org/10.1039/c3ra43846e

Journal Name

Dynamic Article Links ►

Cite this: DOI: 10.1039/c0xx00000x

www.rsc.org/xxxxxx

ARTICLE TYPE

Amphipol-Encapsulated $CuInS_2$/ZnS Quantum Dots with Excellent Colloidal Stability

Matthew Booth,[a] Rebecca Peel,[a] Riitta Partanen,[b] Nicole Hondow,[c] Vlad Vasilca,[b] Lars Jeuken[b] and Kevin Critchley*[a]

Received (in XXX, XXX) Xth XXXXXXXXX 20XX, Accepted Xth XXXXXXXXX 20XX
DOI: 10.1039/b000000x

$CuInS_2$ quantum dots encapsulated in ZnS shells have emerged as less-toxic alternatives to cadmium-based nanoparticles. A well-established synthesis route for hydrophobic CIS/ZnS core/shell QDs has been developed using dodecanethiol as a ligand, solvent and source of sulfur, although the transfer of these nanoparticles into the aqueous phase still proves to be non-trivial. In this study we demonstrate that coating CIS/ZnS with an amphipol, poly(maleic anhydride-alt-1-tetradecene), 3-(dimethylamino)-1-propylamine derivative is an effective method to disperse CIS/ZnS QDs in the aqueous environment. The polymer-coated QDs display good colloidal stability over a wide pH range and low sensitivity to the presence of various metal salts, except Cu^{2+} for which some sensitivity is observed. Cytotoxic effects were tested in HaCat cells and compared to thioglycolic acid modified CdTe/ZnS QDs. Neither CdTe nor CIS QDs decreased viability until above 10 μg/mL in a WST-1 assay. By also assessing the toxicity of the PMAL-d polymer it is clear that remaining toxicity of the CIS/ZnS QDs is predominately due to the polymer coating rather than the QD core. Interestingly, MTT assays seem to artificially exaggerate cytotoxicity of the QDs, which we ascribe to the QDs interfering with the MTT or formazan crystals.

Introduction

The The significant amount of effort invested into the study of cadmium (Cd) based quantum dots (QDs) over the past 30 years has resulted in monodisperse, chemically robust nanoparticles (NPs) with bright, tunable fluorescence that have been advocated for a wide range of applications including lasers, LEDs and solar cells, as well as fluorophores for biological imaging. However, the application of Cd is becoming increasingly restricted by EU regulations designed to limit environmental and health hazards. Current environmental exposure to Cd is already significant enough that urinary Cd levels in the general population approach concentrations where chronic toxicity can be expected.[1] In the case of QDs it has become apparent that Cd can eventually leach out of QDs[2] despite their encapsulation within ZnS[3] or SiO_2[4] shells, or phospholipid micelles,[5] raising environmental and health and safety concerns. A recent study observing primates treated with CdSe QDs did not show any acute toxic effects; however, their spleen, kidneys, and lungs contained raised levels of toxic elements (Cd and Se)[6], which potentially cause chronic toxicity. Many questions still remain regarding nanotoxicity and the possibility for safe use of Cd-based QDs in healthcare applications is doubtful. The task therefore is to develop QDs with similar optical properties (extinction coefficient and photoluminescent quantum yield, PLQY) to Cd-based QDs from elements that are inherently less toxic. Various alternative QD materials are being explored, including InP,[7,8] Ge,[9,10] Si [11,12] and rare earth metal doped ZnS,[13] and much research is focused on analyzing the effect of surface composition on interactions between QDs and cells.[14-17]

Our approach has been to study $CuInS_2$ (CIS) QDs,[18,19] a material that has attracted attention due to its tunable bright emission within the near infrared (NIR)[20-23] and apparent low toxicity in comparison to Cd-based QDs,[24] in addition to a synthesis route that is both cheap and rapid. A layer of ZnS can also easily be formed on the surface, resulting in CIS/ZnS core/shell QDs that are brighter and more stable than core-only CIS QDs.[19-22] However, this synthesis employs dodecanethiol (DDT) as the solvent, sulfur source and critically as the surface ligand, rendering the QDs dispersible in non-polar solvents only.

General strategies for transferring hydrophobic QDs into the aqueous phase include (1) ligand exchange, (2) silanization, (3) coating in lipids, or (4) encapsulation with amphiphilic polymers (amphipols). The exchange of hydrophobic ligands for hydrophilic replacements has been shown to be a successful route towards aqueous stability for various QDs; however, the technique is notoriously problematic. The most promising ligand exchange studies indicate that an anaerobic environment along with precise control over both the solution pH and ligand concentration is necessary for success.[25] In addition, the ligand exchange can cause the ZnS shell to be reduced in thickness, which is likely to cause an increase in the density of surface trap states and thus reduce the PLQY by the promotion of non-radiative recombination pathways. More specifically, in the case of CIS, ligand exchange is less energetically favorable than in the case of exchanging trioctylphosphine oxide (TOPO) stabilized

CdSe/ZnS with a ω-alkanethiol derivative, since DDT has a high binding affinity for ZnS and CIS.

Coating QDs with SiO_2 has been demonstrated by a number of groups.[26-29] The significant advantage of this technique is the low toxicity and inert nature of SiO_2. However, the disadvantage of this approach is the considerable increase in NP diameter and the lack of control over the shell thickness. Furthermore, the technique relies on there being a degree of ligand exchange on the NP surface to seed the formation of the shell. Reports have shown that DDT stabilized zinc doped $AgInS_2$ QDs could be successfully encapsulated into SiO_2 shells to produce NPs that are water soluble and which demonstrate a low cytotoxicity to NIH/3T3 cells.[29]

Tanaka et al. demonstrated that nonanethiol stabilized CIS QDs could be incorporated into the lipid bilayers of vesicles.[18] In this approach the hydrophobic QDs can interact with the hydrophobic chains of the lipids. However, the limited space inside a lipid bilayer (< 4nm) forces an upper size limit on the hydrodynamic radius of the QDs (and therefore the emission wavelength).

Amphiphilic polymers, or amphipols, are a class of surfactant synthesized by grafting hydrophobic chains onto a polymer with a strongly hydrophilic backbone and were developed to stabilize membrane proteins in aqueous solution without the need for detergent.[30] Pellegrino et al. pioneered a novel approach to rendering nanocrystals dispersible in aqueous solutions by encapsulating hydrophobic CdSe/ZnS QDs in an amphipol, specifically poly(maleic anhydride alt-1-tetradecene).[31] The existing hydrophobic ligands on the QD surface were coupled with the long hydrophobic chains of the amphipol through hydrophobic interactions, leaving the polar maleic anhydride (hydrophilic) groups exposed. The creation of a second organic layer as opposed to replacing the first avoids the need for ligand exchange and as a result preserves the QD surface from corrosion and damage. The successful transfer of several hydrophobic NP types into the aqueous phase has been demonstrated by employing various PMAL derivatives,[32-35] amphiphilic PEG polymers[5,36] and alkyl modified poly-acrylic acid.[37-39] Electrostatic interactions have also been utilized in order to encapsulate QDs in polymer, for example between the positively charged side chains of poly(acrylamide) (PAM) and the negatively charged mercapto-acetic acid ligands on the surface of CdSe/ZnS QDs.[40] The photostability of QDs passivated with amphipols has been shown to be significantly improved in comparison to those encapsulated in micelles.[41]

In general, stability in the aqueous environment is achieved through either the presence of polyethylene glycol (PEG) chains or chargeable polar groups. Both methods are effective, yet recent studies have suggested that a zwitterionic surface provides an excellent alternative to PEG since a much lower molecular weight is required in order to achieve good stability.[42,43] In addition, the resistance to non-specific protein adsorption associated with PEG coatings is also observed for zwitterionic alternatives. Furthermore, Zhou et al have demonstrated that gold nanorods with a zwitterionic phosphorylchlorine surface display an enhanced cell uptake specific to cancer cells, in addition to good stability and reduced cytotoxicity (compared to GNRs coated with PEG).[43]

In this study, we encapsulated CIS/ZnS QDs with the commercially available poly(maleic anhydride-alt-1-tetradecene), 3-(dimethylamino)-1-propylamine derivative (PMAL-d), an amphipol derivative of PMAL with equal ratio of carboxylic acids and tertiary amines, to form CIS/ZnS/PMAL-d NPs. Presently there has been only one study that has considered the use of PMAL-d to transfer hydrophobic QDs (TOPO capped CdSe/ZnS) into the aqueous phase to demonstrate the superior transfection properties which arise from the zwitterionic nature of PMAL-d, compared to traditional transfection reagents such as polyethylenimine.[44] Importantly, the CdSe/ZnS/PMAL-d NPs were also observed to have a reduced cytotoxicity to SK-BR-3 cells.

We extend the use of PMAL-d to the water-solubilization of dodecanethiol coated CIS/ZnS QDs and study the stability of the product NP, concentrating on the sensitivity of the optical properties to solution pH and to the presence of various metal ions in solution.

Finally, the cytotoxicity of CIS/ZnS/PMAL-d NPs to a HaCat cell line is evaluated with both MTT and WST-1 assays and compared to thioglycolic-acid (TGA) coated CdTe/ZnS QDs. Whilst in-vivo studies are required to gain a clear idea of the toxicity of NPs at the organism level, in-vitro viability assays can provide useful information about toxicity at the cellular or tissue level. Recently, artifacts have been reported in the results from MTT fluorometric viability assays in cells loaded with single wall carbon nanotubes (CNTs),[45-48] boron nitride nanotubes,[49] as well as iron oxide[50] and TiO_2[51] nanoparticles. These artifacts have been attributed to interactions between the fluorometric agent and the nanomaterials being studied. We observe similar inconsistencies between the results of the two assays performed and conclude that the MTT assay provides inaccurate cell viability data due to interactions between MTT formazan crystals and the QDs. Based on the WST-1 assay the CIS/ZnS/PMAL-d NPs do not significantly reduce cell viability of the HaCat cells until concentrations greater than 10 µg/mL, and by assessing the viability of cells loaded with free PMAL-d only we show that the remaining toxicity can be primarily associated with the polymer coating rather than the CIS/ZnS QD itself.

Experimental Section

Materials Indium (III) acetate (99.99%), copper (I) iodide (99.999%), dodecanethiol (DDT, >98%), zinc stearate (90%), copper (II) chloride, iron (III) acetylacetonate, magnesium (II) sulfate, cobalt (II) chloride, sodium hydroxide, zinc (II) nitrate, cadmium (II) perchlorate, thioglycolic acid (TGA, 98%), and octadecene (ODE, 90%) were purchased from Sigma Aldrich. HPLC grade methanol, chloroform, acetone, nitric acid (70%), hydrochloric acid (32%), and hexane (>97%) were purchased from Fischer Scientific (UK). Poly(maleic anhydride-alt-1-tetradecene), 3-(dimethylamino)-1-propylamine derivative (PMAL-d) was supplied by Sigma Aldrich (MW ~12kDa). 1-(4,5-dimethylthiazol-2-yl)-3,5-diphenylformazan (MTT) was supplied by Sigma. All chemicals were used as received.

Synthesis of CIS/ZnS/DDT QDs CIS QDs were synthesized following methods reported elsewhere.[23] Briefly, 0.1 mmol of copper (I) iodide was placed a three-neck flask. The flask was purged with argon, before the precursors (0.1mmol of indium (III) acetate, and 4 ml of DDT) were heated to 100°C, whilst

Cite this: DOI: 10.1039/c0xx00000x

www.rsc.org/xxxxxx

ARTICLE TYPE

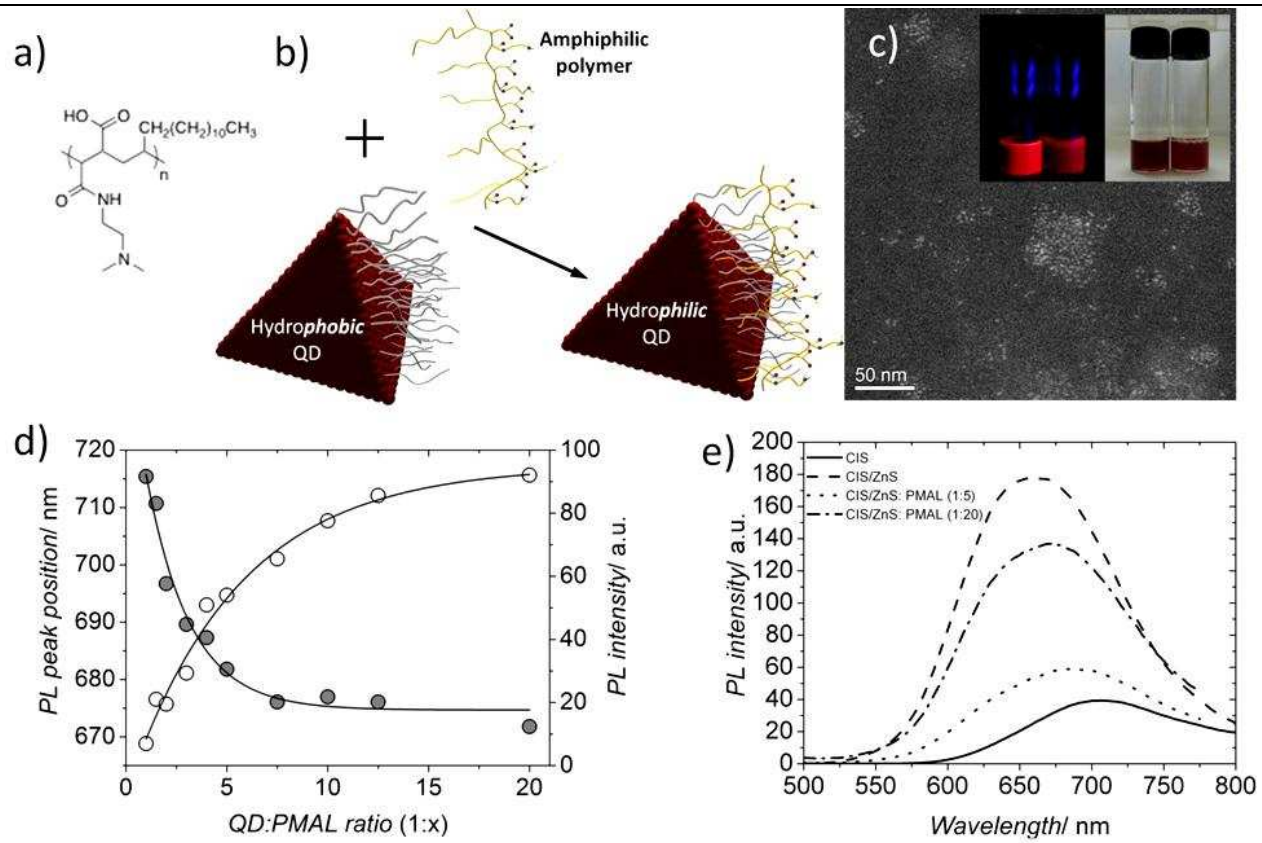

Fig. 1 a) Chemical structure of PMAL-d. b) A cartoon depicting the phase transfer of DDT-capped CIS/ZnS QDs using PMAL-d. c) STEM image of the product, showing primarily single CIS/ZnS/PMAL-d NPs (see Figure S5 in supporting information for high magnification TEM image). Inset: photograph of CIS/ZnS QDs before (left, in hexane) and after phase transfer (right, in deionized water), showing slight red shift in emission. d) PL intensity (hollow circles) and spectral peak position (filled circles) of CIS/ZnS/PMAL-d NPs for molar ratios of QD:PMAL-d for complexation (the lines are guides-to-the-eye). e) PL spectra of CIS/DDT QDs (solid line), CIS/ZnS/DDT QDs (dashed line) and CIS/ZnS/PMAL-d NPs with QD:PMAL-d ratios of 1:5 and 1:20 (dotted and dashed/dotted lines, respectively). All PL spectra were normalised to the absorption at the excitation wavelength, to correct for any variation in concentration between samples.

being continuously stirred. After several minutes the powders were fully dissolved in the DDT and the solution turned a transparent yellow color. The solution temperature was ramped up to 230 °C under argon. The temperature was maintained for a set period of time (5-60 minutes) and then rapidly cooled, the reflux time governing the size of the nanocrystals. In this case, the reflux time was set at 10 minutes to produce ~3 nm QDs. The ZnS shell was formed on the CIS NPs by introducing 0.2 mmol of zinc stearate dissolved in 4 ml of ODE to the as synthesized NPs. The temperature of the solution was raised to 220 °C and maintained for 60 minutes.

Cleaning of the nanoparticles The CIS/ZnS/DDT QDs in hexane were diluted tenfold with a chloroform/methanol/acetone mixture (1:1:10). The solution was then centrifuged at 4000 rpm for 10 minutes at room temperature, resulting in a QD pellet at the bottom of the centrifugation tube. The supernatant was decanted, the QDs were redispersed in hexane and the process was cycled at least three times. The hydrophobic QDs were stored at 8 °C in the dark.

Amphipol encapsulation PMAL-d was dissolved in chloroform (10 mg/mL) and added to the purified CIS/ZnS/DDT QDs dispersion in hexane to give a PMAL-d to QD molar ratio of 20:1 (unless otherwise stated). The solution was stirred vigorously under argon flow for 2 hours and the solvent was evaporated overnight in the dark and at room temperature. Water was added and adjusted to pH 10 by drop wise addition of NaOH. The QDs were dispersed into water by ultrasonicating for 15 minutes.

CIS/ZnS/PMAL-d NP purification The PMAL-d coated QDs were filtered (pore size 0.2 µm) to remove large agglomerates. Free polymer was removed by four cycles of dilution followed by ultra-filtration using Centrisart I (20 kDa supplied by Generon) centrifuge tubes (see supporting information, Figures 1 & 2).

Dynamic Light Scattering and Zeta potential For dynamic light scattering (DLS) experiments a Malvern Zeta Sizer-Nano Series-Zen 3600 was used. A minimum of six measurements was acquired for each sample.

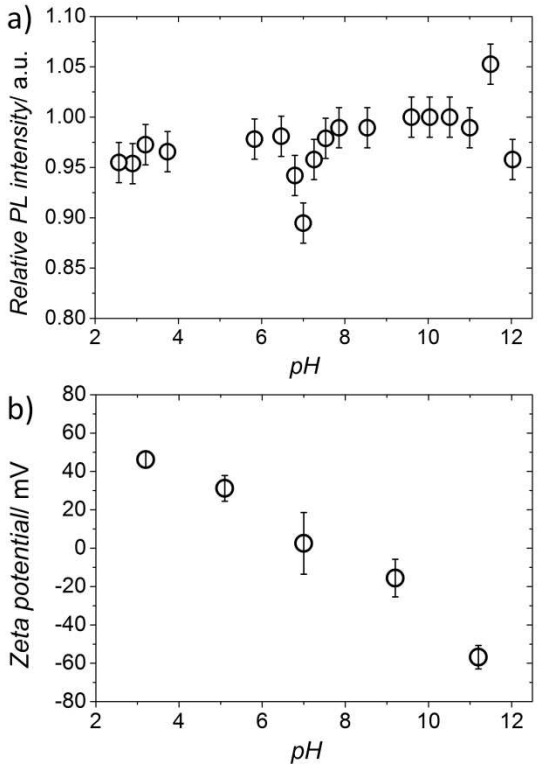

Fig. 2 a) Relative PL intensity of CIS/ZnS/PMAL-d NPs in aqueous solution at various pH levels, normalized to the maximum value of PL intensity at pH 11.5. b) Change in the zeta potential of the CIS/ZnS/PMAL-d NPs over a range of solution pH.

Spectrophotometry and spectrofluoro-photometry The UV-Vis absorption spectra were recorded with a Perkin−Elmer Model Lambda35 spectrophotometer. Photoluminescence (PL) spectra were recorded with a Perkin−Elmer Model LS55 spectrometer fitted with a red-sensitive detector calibrated to the manufacturer's standard. The excitation wavelength was set to 400 nm for all samples and all PL spectra are normalized to the absorption at 400nm.

Scanning Transmission electron microscopy STEM data were acquired using a FEI Tecnai TF20 FEGTEM Field emission gun operated at 200 keV and fitted with HAADF detector and a Gatan Orius SC600A CCD camera. QD samples were dried onto holey carbon films on copper support grids (Agar Scientific, Ltd.).

Synthesis of TGA coated CdTe/ZnS QDs CdTe/ZnS QDs coated in TGA were synthesized following an aqueous synthesis route detailed elsewhere.[52]

Colloidal stability measurements The stability of the CIS/ZnS QDs coated in PMAL-d over a range of pH values was assessed by monitoring the PL intensity as the pH was altered from 12 to 2.5 by drop wise addition of 10 mM HCl to a 10 mM NaOH NP solution.

Cell viability assays HaCat (human keratinocyte) cells were provided by Dr. Routledge (University of Leeds) and cultured in RPMI media (Gibco, Paisley, Scotland) containing 10% fetal calf serum (FCS, Sigma) at 37°C in humidified 5% CO_2. After seeding at a density of 20.000 cells/well in a 96 well plate, HaCat cells were incubated overnight in RPMI and 10% FCS. The spent medium was removed and replaced with fresh RPMI (without FCS) in addition to QDs (or polymer) with concentrations

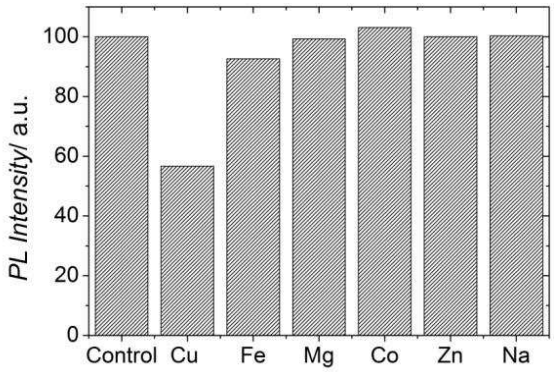

Fig. 3 Relative change in the PL intensity of CIS/ZnS/PMAL-d NPs with emission at 660 nm in 1 mM solutions of various metal ions, normalized to the PL of QDs in water (the control).

ranging from 0.01 to 100 µg/mL and incubated for a further 24 hours. Positive and negative controls were done by omitting the QDs and incubating with 100 µM hydrogen peroxide, respectively. After incubation with the QDs in medium, either a WST-1 or MTT viability assay was performed. The WST-1 (Roche) was performed according the manufacturer's instructions. For the MTT assay, the cells were washed with phosphate-buffered saline PBS (Sigma) and 100 µL MTT1solution (5 mg/mL mg MTT in PBS, filter sterilized) was added to each well (containing 100 µL medium with QDs or PMAL-d). The cells were then incubated for 4 hours, avoiding exposure to light. Each well was topped up with 100 µL of MTT2 (10% SDS (w/v), 10 mM HCl) and incubated overnight at 37 °C. The optical absorbance at 540 nm was measured with plate reader and the results expressed as percentage viability compared with untreated cells. Because in the MTT assay, the QDs remain in the well during the assay, control experiments where performed without HaCat cells to determine the light dispersion and adsorption due to the QDs. These 'background' values became significant at 10 and 100 µg/mL QDs and the background was subtracted from the viability assay data (as a result, cell viability data for the MTT assay can have values slightly below 0%).

Results and discussion

The synthesis procedure (see Experimental Section) resulted in CIS/ZnS/DDT QDs that were dispersed in hexane and CIS/ZnS/PMAL-d NPs that were dispersed in the aqueous phase **(Figure 1)**. Optimization of the molar ratio of QD:PMAL-d used in the encapsulation process was achieved by examining the optical properties of the NP product with QD:PMAL-d: ratios ranging from 1:1 to 1:20. With increasing amounts of polymer (relative to QD), both the integrated PL intensity and the peak emission wavelength of the CIS/ZnS/PMAL-d NPs tended towards that of the as synthesized CIS/ZnS/DDT QDs dispersed in hexane. This is an indication that once the PMAL-d concentration is high enough, this method enables single polymer encapsulated QDs to be dispersed into water. However, for lower quantities of PMAL-d to QDs, a red shift is observed indicating that clusters of QDs are coated in polymer. In this situation, the QDs will be in close enough proximity to undergo Förster-type resonance energy transfer (FRET); energy is transferred from smaller to larger QDs, resulting in lower PLQY and a red shift of

Cite this: DOI: 10.1039/c0xx00000x

www.rsc.org/xxxxxx

ARTICLE TYPE

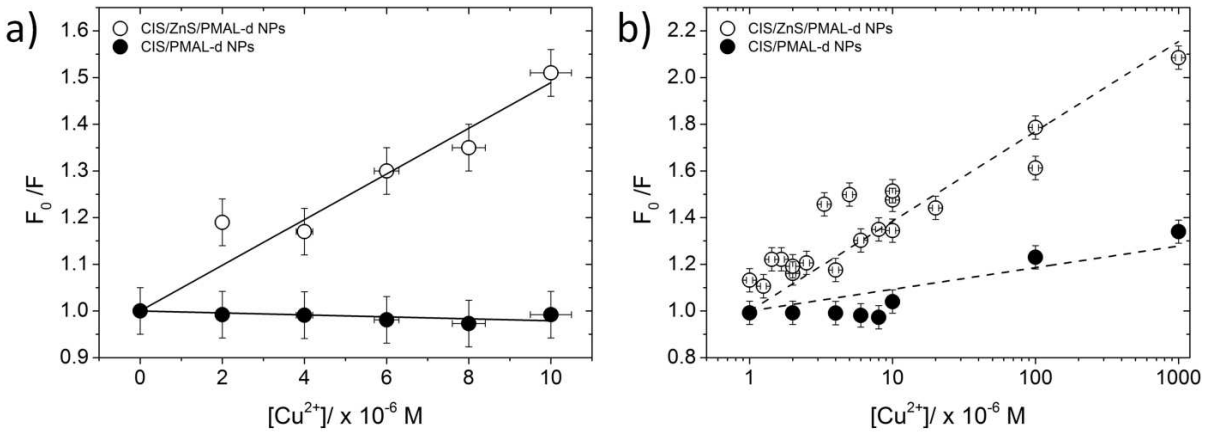

Fig. 4 Relative change in the PL intensity of CIS/ZnS/PMAL-d NPs at 660nm (filled circles) and CIS/PMAL-d NPs at 710nm (filled triangles) in the presence of Cu^{2+} ions. a) The low concentration data were fitted (solid lines) to a modified Stern-Volmer (Eq. 1) The high concentration range is presented on a logarithmic scale (dashed lines are a guide to the eye).

the PL emission wavelength. Unless stated otherwise a PMAL-d:QD molar ratio of 20:1 was used for the encapsulation process which approximately equates to 0.5 polymers per nm^2 of QD surface area (or 15 monomer units per nm^2). This is a lower concentration than suggested by the general method used for the PMAL polymer in Pellegrino et al.'s report; however, this article also stated that as low as 10 monomer units per nm^2 led to successful phase transfer.[30] It should be highlighted that unlike poly(maleic anhydride alt-1-tetradecene), PMAL-d does not require a cross-linker to form stable colloidal dispersions in the aqueous phase. An electron micrograph of the purified PMAL-d coated QDs deposited onto a transmission electron microscope (TEM) grid confirmed that the NPs consist of individual QDs rather than clusters (Figure 1c).

The hydrodynamic diameter of the CIS/ZnS/PMAL-d NPs was determined by dynamic light scattering (DLS) to be 13.7 ± 3.2 nm at neutral pH and was found to be constant over the entire pH range studied within experimental error (see supporting information, Figure S3). The fluorescence intensity of the NP solution was monitored over the same range of pH **(Figure 2a)**. The relative intensity was found to be stable over a wide range of pH except for a narrow 10% dip in intensity close to neutral pH. At pH 11, the zeta potential of the QDs was measured to be approximately -60 mV (Figure 2b), and thus can be defined as a highly stable charged colloidal dispersion. At pH 3, the QDs were found to be positively charged with a zeta potential of approximately 50 mV, also indicative of a highly stable dispersion. As the pH tended towards neutral, the zeta potential magnitude decreased with an apparent isoelectric point at approximately pH 7. This trend can be explained by the zwitterionic nature of PMAL-d. At high pH the carboxylic acid becomes deprotonated resulting in a net negative charge, whilst at low pH the tertiary amine become protonated resulting in a net positive charge. However, at neutral pH, the electrostatic repulsion between NPs will be weak and the colloidal stability is lowered (with only steric hindrance of the thick polymer layer contributing) explaining the small decrease in relative fluorescence intensity observed (Figure 2a).

The CIS/ZnS/PMAL-d NPs were dispersed in aqueous solutions containing metal ions to determine whether specific ions caused fluorescence quenching. The only solution which caused significant quenching of the PL emission (approaching 50% for a 1mM solution) was Cu^{2+} **(Figure 3)**.

Given that the optical absorption from Cu^{2+} (in solution) overlaps with the QD fluorescence maximum (650-720 nm, see supporting information), it would be possible that the observed decay in fluorescence from the NPs was due to the emitted photons being absorbed directly by the Cu^{2+} in solution, or that an energy transfer process was occurring. However, if this were the case, the effect would be enhanced in the CIS/PMAL-d NPs, because their emission maximum is better matched to the Cu^{2+} absorption band than the CIS/ZnS/PMAL-d NPs (see supporting information, Figure S4). In fact, the quenching effect is stronger in the CIS/ZnS/PMAL-d NPs and therefore we can conclude that absorption by the Cu^{2+} in solution produces a negligible contribution to the observed quenching.

To investigate the mechanism behind the quenching effect further, static and dynamic quenching were modeled using the Stern-Volmer relationship,[53] which describes a linear relationship between the concentration of the quencher $[Q]$ and the relative decrease in fluorescence intensity. This relationship holds for CIS/ZnS/PMAL-d NP dispersions in the presence of low concentrations of Cu ions but not for high concentrations **(Figure 4)**.

Similar non-linear quenching is observed in systems where the quencher has limited accessibility to the fluorophore,[53] and can be modeled by considering a modified Stern-Volmer expression,

$$\frac{F_0}{F_0 - F} = \frac{1}{f_a K_a [Q]} + \frac{1}{f_a} \qquad (1)$$

where F_0 is the fluorescence intensity in the absence of the

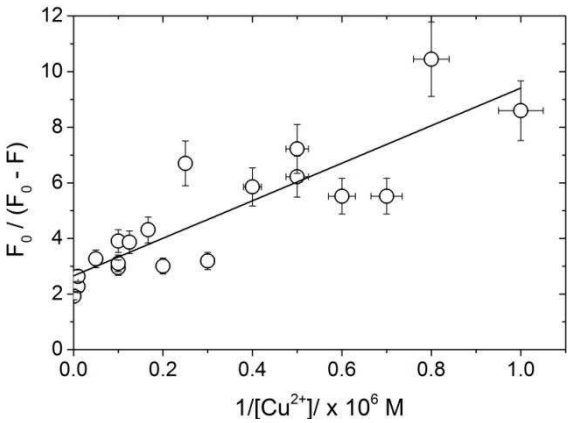

Fig. 5 The CIS/ZnS/PMAL-d data were plotted to enable the evaluation of the modified-Stern-Volmer model (Eq. 1). The solid line is the line of best fit.

quencher Q (in this case Cu^{2+}), F is the fluorescence intensity in the presence of Q, f_a is the fraction of fluorophores which are accessible to Q, and K_a is the Stern-Volmer coefficient for the accessible fraction. Fitting Eq. 1 to the CIS/ZnS/PMAL-d data was achieved by plotting $F_0/(F_0\text{-}F)$ against $1/[Cu^{2+}]$ **(Figure 5)**. A line of best fit gives an intercept and a gradient of 2.7 ± 0.4 and 6.8 ± 0.9 × 10^{-6} M, respectively. The intercept corresponds to $1/f_a$, which implies that the percentage of QDs accessible to the quencher was 37 ± 6 %. We speculate that the combination of the DDT ligands and the thick PMAL-d layer around the CIS/ZnS QDs form an effective barrier to the Cu^{2+} ions in the majority of the sample (~63%); however, ~37% are not fully protected and can allow Cu^{2+} ions to interact with the QDs. The gradient corresponds to the Stern-Volmer coefficient of the accessible fraction and in the case of CIS/ZnS/PMAL-d NPs K_a was estimated to be 4.0 ± 0.2 × 10^5 M^{-1}. This large Stern-Volmer coefficient highlights the relatively high sensitivity of CIS/ZnS/PMAL-d to Cu^{2+} ions.

Surprisingly, the CIS/PMAL-d NPs were found to be less sensitive to Cu^{2+} ions (Figure 4). Fitting the CIS/PMAL-d data to the modified Stern-Volmer equation (Eq. 1), estimates the accessible percentage to be 29 ± 3 % with a Stern-Volmer coefficient, K_a, of 1.4 ± 0.1 × 10^4 M^{-1}; the core QDs displayed an order of magnitude lower sensitivity to Cu ions than the core-shell QDs.

Quenching of QD fluorescence in the presence of Cu^{2+} ions has been observed for CIS QDs[54] as well as for other QD systems[55,56] and the quenching mechanism is still under debate. Reports suggest that that the Cu^{2+} ions can react with the ZnS surface of core-shell QDs creating Cu_xS_y, which lead to increased density of surface trap states. Another possible explanation is that Cu^{2+} complexes with the QD resulting in a non-radiative recombination pathway. However, for the CIS/ZnS/PMAL-d system, the quenching behavior indicates that only a fraction of the QDs are affected. Quenching caused by complexation of Cu^{2+} at the surface seems less likely given that the organic chemistry of both CIS/ZnS and CIS are identical (and therefore we would expect a similar response to the quencher). It seems more likely that the Cu^{2+} ions react with the ZnS surface and form surface trap states which reduce the PL intensity. This explanation is

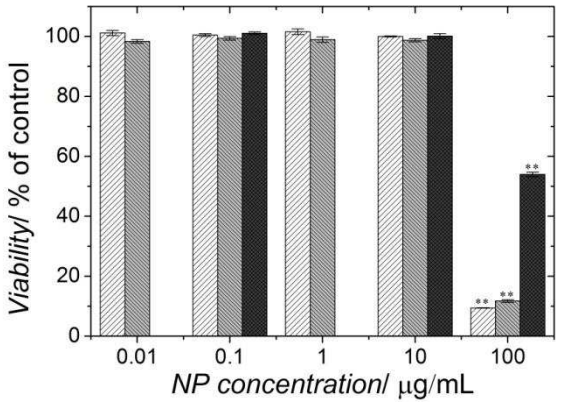

Fig.6 Cell viability of HaCat cells loaded with CIS/ZnS/PMAL-d NPs (white dashed bars), free PMAL-d (grey dashed bars) and TGA coated CdTe/ZnS QDs (dark grey dashed bars), from a WST-1 cell viability assay. Error bars represent the S.E. ($*p < 0.01$, $**p < 0.001$).

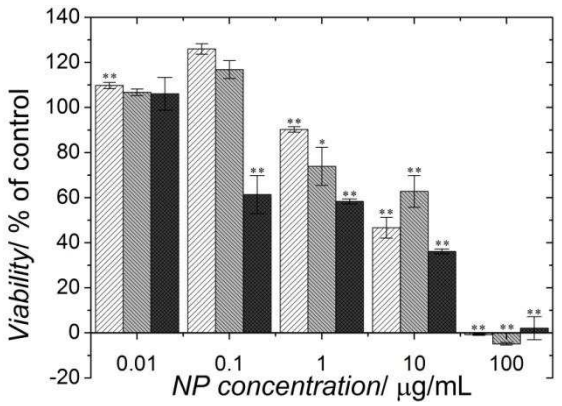

Fig. 7 MTT cell viability assay results for HaCat cells loaded with CIS/ZnS/PMAL-d NPs (white bars), free PMAL-d (grey bars) and TGA coated CdTe/ZnS QDs (black bars). Error bars represent the S.E. ($*p < 0.01$, $**p < 0.001$).

consistent with the fact that Cu^{2+} ions have less of a quenching effect on core CIS QDs; CIS QDs already have high densities of surface trap states compared to CIS/ZnS QDs.[19,23]

The effect of the CIS/ZnS/PMAL-d NPs on the viability of HaCat cells was assessed in vitro using both a WST-1 assay and an MTT assay. The cytotoxicity of CIS/ZnS/PMAL-d NPs were compared to that of TGA coated CdTe/ZnS QDs and free PMAL-d (at concentrations corresponding to the amount of PMAL-d estimated to be present in each of the CIS/ZnS/PMAL-d NP concentrations). According to the WST-1 assay, the NPs do not reduce cell viability up to and including concentrations of 10 μg/mL **(Figure 6)**. Viability assay with PMAL-d on its own suggested that the observed CIS/ZnS toxicity at 100 μg/mL can be attributed PMAL-d, although further studies comparing the cell viability of cells loaded with CIS/ZnS QDs encapsulated in a variety of polymers are needed to confirm this. It is likely, however, that all amphiphilic polymers will have some influence on cell viability.

The cytotoxicity of CIS/ZnS/PMAL-d NPs seems to be comparable to that of TGA coated CdTe/ZnS QDs. However, we note that the health concern with Cd-based QDs is not that they might cause acute toxic effects but that accumulation of Cd ions

in the vital organs, as seen in vivo, may generate severe chronic toxic effects.[6] It is the chronic toxicity associated with Cd-based QDs which the development of Cd-free QDs such as CIS aims to avoid.

Interestingly, the MTT assay shows a very distinct behavior compared to the WST-1 assay **(Figure 7)**. At low concentrations of CIS/ZnS/PMAL-d NPs, viability seems to improve, which is partly caused by the PMAL-d. However, at higher concentrations, the viability seems to decrease in a two-step manner. Between 0.1-10 μg/mL (the first step), viability is approximately halved, while at 100 μg/mL, a second 'step' in viability loss is observed. This is inconsistent with the WST-1, which shows full viability up to 10 μg/mL. We note that in the MTT assay, the PMAL-d or QDs remain present in the MTT mixture during the assay and we propose that the discrepancy between the two assays is due to artifacts induced by interactions between the NPs and the tetrazolium MTT dye or formazan, a phenomenon which has previously been reported in the literature for various nanostructures.[43-49]

Conclusions

High quality CIS/ZnS QDs were transferred to the aqueous phase by wrapping amphipols around the QDs. The method was optimized by monitoring the PL intensity and the spectral peak position whilst the QD:polymer molar ratio was changed. The hydrodynamic diameter of the resulting NPs was approximately 10 nm, which is significantly larger than the 4 nm for the hydrophobic DDT coated QDs. This is consistent with polymer encapsulated QDs suggesting that each NP consists of a single QD wrapped in polymer. Colloidal stability was promoted by the zwitterionic properties of PMAL-d; carboxylic acid groups provide a large negative zeta potential at high pH and tertiary amine groups provide a positive zeta potential at low pH. This strong charge repulsion between the NPs rendered them stable in water between pH 2 and pH 12, with a minimum in stability at approximately neutral pH. The stability of the NPs in the presence of various cations was investigated with only Cu^{2+} producing a significant quenching effect. Because of the non-linear relationship between quencher concentration and the relative decrease in fluorescence intensity, as well as the increased sensitivity of the CIS/ZnS/PMAL-d compared to CIS/PMAL-d NPs, we conclude that the quenching mechanism is the formation of surface trap states as a result of the reaction between Cu ions and the ZnS surface, and that this process is limited by the thick organic layer of the polymer coating.

The in-vitro effect of CIS/ZnS/PMAL-d NPs on HaCat cells was assessed by means of an MTT assay and a WST-1 assay. The observed cell viability of the cells was dependent on the chosen assay; the MTT assay seems to artificially exaggerates the reduction in cell viability, probably due to an interaction between the NPs and MTT formazan crystals and similar to that observed with CNTs by Wörle-Knirsch et al.[43] Our results reiterates that care has to be taken when interpreting 'classical' cell viability assays in the field of nanotoxicology and that multiple cell viability assays need to be compared, a practice that is more often than not disregarded in QD studies.

In conclusion, the encapsulation of CIS/ZnS QDs with PMAL-d produces water dispersible NPs that display excellent colloidal stability over a wide pH range, and comparatively low susceptibility to quenching by ions in solution (with the exception of Cu^{2+}). Although the inherently low toxicity of CIS QDs in comparison to CdTe QDs is partly counteracted by the inherent toxicity of the PMAL-d, and these NPs are suitable for in vitro cell imaging and labeling at concentrations up to and including 10 μg/mL. In order to further develop this system towards in vivo or clinical applications, more work will be necessary to tune the surface chemistry to reduce toxicity.

Acknowledgements

This work was financially supported by the BHRC (University of Leeds), ESPRC (EP/J01513X/1 and EP/K023845/1) and the Royal Society. LJ and RP received funding from the European Research Council under the European Union's Seventh Framework Programme (FP/2007-2013)/ERC Grant Agreement n. 280518. NH is supported by a AXA research fellowship. The authors thank Prof. S. D. Evans and Prof. R. J. Bushby for useful discussions.

Notes and references

a School of Physics& Astronomy, University of Leeds, Leeds, UK. E-mail: K.Critchley@leeds.ac.uk
b School of Biomedical Sciences, University of Leeds, Leeds, UK.
c Institute for Materials Research, University of Leeds, Leeds, UK

† Electronic Supplementary Information (ESI) available: Further details of the purification procedure, dynamic light scattering data for determination of hydrodynamic diameter, absorption spectrum for Cu^{2+} in solutionand high resolution TEM image of CIS/ZnS/PMAL-d NP .See DOI: 10.1039/b000000x/

1 K. T. Yong, W. Law, R. Hu, L. Ye, L. Liu, M.T. Swihart, P.N. Prasad, Chem. Soc. Rev., **2013**, 42, 1236
2 A.M. Derfus, C.W.C. Chan, S.N. Bhatia, Nano Letters **2004**, 4, 11-18
3 C. Kirchner, T. Liedl, S. Kudera, T. Pellegrino, A.M. Javier, H.E. Gaub, S. Stölzle, N. Fertig, W.J. Parak, Nano Letters **2005**, 5, 331-338
4 S.T. Selvan, T. T. Tan, J.Y. Ying, Adv. Mater. **2005**, 17, 1620-1625
5 B. Dubertret, P. Skourides, D.J. Norris, V. Noireaux, A. H. Brivanlou, A. Libchaber, Science, **2002**, 298, 1759
6 L. Ye, K.T. Yong, L. Liu, I. Roy, R. Hu, J. Zhu, H. Cai, W.C. Law, J. Liu, K. Wang, J.Liu, Y. Liu, Y. Hu, X. Zhang, M.T. Swihart, P.N. Prasad, Nature Nanotechnology, **2012**, 7, 453-458
7 D.W. Lucey, D.J. MacRae, M. Furis, Y.Sahoo, A.N. Cartwright, P. N. Prasad, Chem. Mater. **2005**, 17, 3754-3762
8 R. Xie, D. Battaglia, X. Peng, J. Am. Chem. Soc. **2007**, 129, 15432-15433
9 D.A. Ruddy, J.C. Johnson, E.R. Smith, N.R. Neale, ACS Nano **2010**, 12, 7459-7466
10 D.C. Lee, J.M. Pietryga, I. Robel, D.J. Werder, R.D. Schaller, V.I. Klimov, J. Am. Chem. Soc. **2009**, 131, 3436–343
11 F. Erogbogbo, K.T. Yong, R.Hu, W.C. Law, H. Ding, C.W. Chang, P.N. Prasad, M.T. Swihart, ACS Nano **2008**, 5, 873-878
12 Y. He, Z.H. Kang, Q.S. Li, C.H.A. Tsang, C.H. Fan, S.T. Lee, Angew. Chem. Int. Ed. **2009**, 48, 128–132
13 K. Manzoor, S. Johny, D. Thomas, S. Setua, D. Menon, S. Nair, Nanotechnology **2009**, 20, 065102 2009
14 V.V. Breus, C.D. Heyes, K. Tron, G.U. Nienhaus, ACS Nano. **2009**, 3, 2573–2580
15 T.A. Kelf, V.K.A Sreenivasan, J. Sun, E.J. Kim, E.M. Goldys A.V. Zvyagin, Nanotechnology, **2010**, 21, 285105
16 E.L. Bentzen, I.D. Tomlinson, J. Mason, P. Gresch, M.R. Warnement, D.Wright, E. Sanders-Bush, R. Blakely, S.J. Rosenthal, Bioconjug. Chem., **2005**, 16, 6, 1488-94

17 B.A. Kalrdolf, M.C. Mancini, A.M. Smith, S. Nie, Anal. Chem., **2008**, 80, 8, 3029-34
18 M. Tanaka, K. Critchley, T. Matsunaga, S.D. Evans, S.S. Staniland, Small, **2012**, 8, 10, 1590-5
19 M. Booth, A.P. Brown, S.D. Evans, K. Critchley, Chem. Mater., **2012**, 24, 11, 2064–2070
20 L. Li, T.J. Daou, I. Texier, T.T. Kim Chi, N. Q. Liem, P. Reiss, Chem. Mater. **2009**, 1, 2422-2429
21 K. T. Yong, I. Roy, R. Hu, H. Ding, H. Cai, J. Zhu, X. Zhang, E.J. Bergey, P.N. Prasad, Integr. Biol., **2010**, 2, 121-129
22 J. Park, S.W. Kim, J. Mater. Chem. **2001**, 21, 3745-3750
23 L. Li, A. Pandey, D.J. Werder, B.P. Khanal, J.M. Pietryga, V.I. Klimov, J. Am. Chem. Soc. **2011**, 133, 1176–1179
24 T. Pons, E. Pic, N. Lequeux, E. Cassette, L. Bezdetnaya, F.Guillemin, F. Marchal, B. Dubertret, ACS Nano **2010**, 4, 2531-2538
25 S. Tamang, G. Beaune, I. Texier, P. Reiss, ACS Nano, **2011**, 5, 12, 9392-9402
26 M.Q. Zhu, J.J Han, A.D. Li, J. Nanosci. Nanotechnol., **2007**, 7, 2343-8
27 C. Lai, Y.H. Wang, Y.C. Chen, C.C. Hsieh, B.P. Uttam, J.K. Hsiao, C.C. Hsu, P.T. Chou, J. Mater. Chem., **2009**, 19, 8314–8319
28 L. Jing, Y. Li, K. Ding, R. Qiao, A.L. Rogach, M. Gao, Nanotechnology, **2011**, 22, 505104
29 Y. Sheng, X. Tang, J. Xue, J. Mater. Chem., **2012**, 22, 1290
30 C. Tribet, R. Audebert, J. Popot, Proc. Natl. Acad. Sci. USA, **1996**, 93, 15047-15050
31 T. Pelligrino, L. Manna, S. Kudera, T. Liedl, D. Koktysh, A.L. Rogach, S. Keller, J. Rädler, G. Natile, W.J. Parak, Nano Lett., **2004**, 4, 4, 703-707
32 E.E. Lees, T.L. Nguyen, A.H.A. Claton, P. Mulvaney, ACS Nano, **2009**, 3, 5, 1121-1128
33 C. Zhou, H. Shen, Y. Guo, L. Xu, J. Niu, Z. Zhang, Z. Du, J. Chen, L.S. Li, J. Colloid and Interface Science, **2010**, 344, 279-285
34 H. Duan, M. Kuang, Y.A. Wangi, Chem. Mater., **2010**, 22, 4372-4378
35 S.A. Diaz, G.O. Menendez, M.H. Etchehon, L. Giordano, T.M. Jovin, E.A. Jares-Erijman, ACS Nano, **2011**, 5, 4, 2795-2805
36 W.W. Yu, E. Chang, J.C. Falkner, J. Zhang, A.M. Al-Somali, C.M. Sayes , J. Johns, R. Drezek, V.L. Colvin, J. Am. Chem. Soc., **2007**, 129, 2871-2879
37 X. Wu, H. Liu, J. Liu, K.N. Haley, J.A. Treadway, J.P. Larson, N. Ge, F. Peale, M.P. Bruchez, Nature biotechnology, **2002**, 21, 41-46
38 C. Luccardini, C. Tribet, F. Vial, V. Marchi-Artzner, M. Dahan, Langmuir, **2006**, 22, 2304-2310
39 R.E. Anderson, W.C. Chan, ACS Nano, **2008**, 2, 7, 1341-1352
40 I. Potapova, R. Mruk, S. Prehl, R. Zentel, T. Basche, A. Mews, J. Am. Chem. Soc., **2003**, 125, 320-321
41 D.L. Nida, N. Nitin, W. W. Yu, V. L. Colvin, R. Richards-Kortum, Nanotechnology, **2008**, 19, 035701
42 A. J. Keefe, S. Jiang, Nature Chemistry, **2012**, 4, 59-63
43 W. Zhou, J. Shao, Q. Jin, Q. Wei, J. Tang, J. Ji, Chem. Commun., **2010**, 46, 1479–1481
44 L. Qi, X. Gao, ACS Nano, **2008**, 2, 7, 1403-1410
45 J.M. Wörle-Knirsch, J. Pulskamp, H.F. Krug, Nano Letters, **2006**, 6, 6, 1261-1268
46 A. Casey, E. Herzog, M. Davoren, F.M. Lyng, H.J. Byrne, G. Chambers, Carbon., **2007**, 45, 1425–1432.
47 M. Davoren, S.P. Mukherjee, H.J. Byrne, Toxicol. In Vitro, **2007**, 21, 438–448.
48 E. Herzog, A. Casey, F.M. Lyng, G. Chambers, H.J. Byrne, M. Davoren, Toxicol. Lett., **2007**, 174, 49–60.
49 G. Ciofani, D. Serena, G.G. Genchi, D. D'Alessandro, J. Pellequer, M. Odorico, V. Mattoli, M. Giorgi, Biochem. Biophys. Res. Commun., **2010**, 394, 405-411.
50 S.M. Griffiths, N. Singh, G. J. S. Jenkins, P. M. Williams, A. W. Orbaek, A. R. Barron, C. Wright, S. H. Doak, Anal chem., **2011**, 83, 3778-3785
51 A.L. Holder, R. Goth-Goldstein, D. Lucas, C.P. Koshland, Chem. Res. Toxicol., **2012**, 25, 1885−1892
52 S.A. Peyman, R.H. Abou-Sale, J.R. McLaughlan, N. Ingram, B.R.G. Johnson, K. Critchley, S. Freear, J.A. Evans, A.F. Markham, P.L. Coletta, S.D. Evans, Lab on a Chip, **2012**, 12, 4544-4552
53 J.R. Lakowicz, Principles of Fluorescence Spectroscopy, 2nd Ed.; Kluwer Academic Plenum Publishers, New York, **1999**
54 S. Liu, Y. Li, X. Su, Anal. Methods, **2012**, 4, 1365-1370
55 A.V. Isarov, J. Chrysochoos, Langmuir, **1997**, 13, 3142-3149
56 S. Ghosh, A. Priyam, S.C. Bhattacharya, J. Fluoresc., **2009**, 19, 4, 723-731